Contamination is not the only way to slow down rising air bubbles

Mingming Wu

Department of Physics, Occidental College, Los Angeles, CA 90041, USA

Morteza Gharib

Graduate Aeronautical Laboratories, California Institute of Technology, Pasadena, CA 91125, USA

(January 16, 2001)

Abstract

It is known that air bubbles rising in water can be slowed down significantly with the addition of a minute amount of contamination in water. We find, in clean water, bubbles can be slowed down the same magnitude by using a different bubble generation mechanism. We present experimental studies on the path and shape of single air bubble (diameter range of $0.10 - 0.20cm$) rising freely in clean water. Experimental results show that bubbles' shape can be either sphere or ellipsoid depending on its generation mechanism. The spherical bubbles move significantly slower than the ellipsoidal ones of the same volume. Furthermore, we find that the straight path of a spherical bubble changes to a zigzag path; while the straight path of an ellipsoidal bubble changes to a spiral path when the Reynolds number exceeds a threshold.

PACS numbers: 47.55.Dz, 47.20.-k, 47.27.Vf

The study of the motion of rising air bubbles in various fluids has been the subject of a large amount of work during the last century (for a review, see Clift, Grace and Weber [1], and a recent review article by Magnaudet and Eames [2]). One principal reason for the attention given is the simplicity of its geometry, and it represents an important class of free boundary problem in fluid dynamics [3]. In addition, it affords an opportunity to study two poorly understood phenomena in fluid dynamics, wake instabilities [4] and flow separation near a free surface [5]. On the practical side, the basic understanding of the motion of single air bubble is essential for the understanding of two phase flows that often occur in nature and various industrial processes.

One of the fascinating problems on the motion of air bubbles is the effect of surface-active contaminants [1,6,7]. It is known that the terminal velocity of the air bubble decreases significantly with the addition of a minute amount of contaminant in water. This phenomena is currently best understood by a stagnant-cap model, where the surfactant molecules are swept to the rear of the bubble surface and form a stagnant cap. The rigidity of the stagnant cap leads to the increase of the shear stress around the surface of the bubble, and thus, the decrease of the rising velocity. In Fig. 1, the upper dashed line is experimental data obtained in clean water by Duineveld [8], and the lower solid line is data taken in water saturated with contaminants [1]. It is shown that bubbles rise much slower in contaminated water. This phenomena is especially prominent in the bubble diameter regime of 0.1 - 0.2 cm [1]. The velocity versus diameter curves obtained by various investigators in this diameter regime differ somewhat, and generally lie along these two lines in Fig. 1 (For a detailed comparison, see Fig. 7.3 of Ref.[1]). While some of the spread among the data results from experimental errors, the greatest cause is the contamination in water.

In this Letter , we report that, in addition to the cleanness of the water, bubble generation mechanism plays an equally important role in the motion of air bubbles. We studied the path and shape of air bubbles rising in clean water using two different generation mechanisms. Experimental results show that, in clean water, air bubbles in the previously known ellipsoidal regime (0.1 - 0.2 cm) [1] have two stable shapes, a spherical and an ellipsoidal

shape, depending on its generation mechanism. The terminal velocities of spherical bubbles are significantly slower than those of ellipsoidal ones.

The main part of the experimental apparatus is the Plexiglas water tank with dimensions of $6'' \times 6'' \times 24''$, which is large enough to neglect the wall effect [7]. At the center of the bottom plate, a specially designed fitting is mounted for the insertion of a glass capillary tube or a hypodermic needle. The bubble is released through the capillary tube or the hypodermic needle. A high speed camera (1000fps, Kodak Ektapro Motion Analyzer, Model 1000 HRC) is used to take close-up images of the bubble. The camera typically takes an image of 512 pixel $\times$384 pixel with a viewing window of 1.84 cm $\times$ 1.38 cm, in which the lower bound is $\sim$ 2.0 cm above the needle tip. The second camera is a specially designed 3D imaging system, and it is used to map out the (x, y, z) coordinates of the bubble. Here x and y are lateral positions of the bubble, and z is the vertical distance above the needle. The camera obtains z using a quantitative defocusing mechanism [9]. A typical viewing window of the 3D imaging system is 1.5 cm $\times$ 1.5 cm $\times$ 20 cm, in which the lower bound is at least $\sim$ 20 cm (or $\sim$ 100d, d is the bubble diameter) above the needle tip. It needs to be noted that the 3D imaging system is designed in such a way that the spatial resolution in the x-y plane is about 40 times better than the resolution along the z direction, making it an ideal instrument for recording trajectories with small lateral movements. In the current setting, the lateral spatial resolution is 0.005 - 0.01 cm and the vertical resolution is 0.02 - 0.4cm, where the resolution varies with the distance between the bubble and the camera. Extreme caution is taken to keep the tank as clean as possible. Once the tank is filled with water, it is sealed immediately with plastic sheets. Air filters (VWR Scientific, 0.20 μ m) are installed at the air entrance to the bubble generation mechanism and the two ventilation holes at the top of the water tank. The temperature of the water during the experiment is 22 ± 0.3^{o}C.

For the data reported in this paper, we used clean water from a lab in the chemistry department, Occidental College. The water is first taken from a deionized water source of the chemistry building, which has been pretreated by a Culligan water purification system [10]. It is then distilled by an autodistiller (Wheaton split-stream D-10N), and filtered by

a 3-module filtration system (Nanopure, Barnstead) in the lab. The surface tension of the water is 72.8dyn/cm at 21.8^{o}C measured with a Fisher Scientific tensiometer (Tensiomat Model 21). Experiments are also carried out using water from the chemistry department at Caltech, in which the water is filtered with a 4-module filtration system (Nanopure, Barnstead) with specific resistance of $\sim$18 MΩ·cm. Experimental results are consistent with the results presented below.

The bubble generation mechanisms are illustrated in Fig. 2. For the pinch-off method (See Fig. (2a)), air comes in from syringe pump one, passes through a L-shape capillary (8 μl volume, 0.15 cm diameter) and forms a bubble at the tip of a hypodermic needle. The bubble detaches naturally from the needle due to buoyancy force. The bubble size depends on the needle size as well as the shape of the needle tip. For the bubble to detach naturally from the needle, the inner diameter of the needle d_i needs to be much smaller than the bubble diameter d. In our case, d_i ranges from 0.031 - 0.044 cm. In the gentle-push method, we use a glass capillary tube of d_i = 0.123 cm, which is comparable to the bubble size. Due to the large inner diameter of the needle, an extra push is needed for the air bubble to detach from the needle. The following is a typical procedure for generating a bubble using gentle-push method. First, the L-shape capillary is placed in the position shown in Fig. (2b), and water is extracted to the syringe from the water tank. Second, the L-shape capillary is switched to the position shown in Fig. (2a) and a small volume of air is displaced into the L-shape capillary using syringe pump one. Third, the capillary is switched back to the position in Fig. (2b), and the air bubble is pushed out by the syringe filled with water at a very slow rate, typically 0.01 ml/min by syringe pump two. Note that the main difference of these two methods is the size of the needle, pinch-off method requires that $d_i << d$, and gentle-push method requires $d_i \sim d$.

Fig. 3 shows time series of images at the moment of detachment using two different generation methods. In the case of pinch-off method, a thin neck is formed at the rear of the bubble - the point of detachment. This curvature singularity gives rise to a strong axisymmetric surface wave, which in turn propels the bubble to a large initial speed. The

bubble shape reaches a steady shape at a distance of $\sim 1cm$ above the needle tip. Using images taken by the high speed camera, we find that the aspect ratio χ of the bubble (long axis versus short axis) ranges from 1.2 - 2.6 in the bubble diameter regime of 0.1 - 0.2 cm. The measured curve of χ versus Weber number is consistent with that obtained by Duineveld [8]. In the case of gentle-push method(see Fig. 3), the bubble keeps its spherical shape due to the weak perturbations from the detachment process. The spherical bubble gains a slower initial velocity as seen in Fig. 3. The aspect ratio of the bubbles ranges from 1.0 - 1.05 in the bubble diameter regime of 0.1 - 0.2 cm. We also placed the high speed camera at a distance of $\sim$ 20 cm above the needle, and observed no significant shape change.

For a typical experimental run, a series of 60 images is recorded at a rate of 60 images per second using the 3-D camera. Each image contains information necessary for inferring the (x,y,z) coordinates of the bubble. The trajectories of the bubbles are then extracted from the image series. The vertical displacement z of the bubble versus time t is shown in Fig. 4. The vertical velocity U of the bubble is obtained from a linear fit to the experimental data (see solid lines in Fig. 4).

The velocity versus diameter d of our experimental data is shown in Fig. 1. The velocity curve of ellipsoidal bubbles agrees well with previous measurements in clean water, which indicate that our water is clean. On the other hand, the velocity curve of spherical bubbles, *that rise in the same batch of water as the ellipsoidal ones*, is close to previous velocity curve of bubbles rising in water saturated with contaminants.

The trajectories of the bubbles from these two generation mechanisms exhibits some fascinating features. Previously, both spiralling and zigzagging bubbles have been observed in this diameter regime [11,7,12–14,8,15,16], however various experiments are not in agreement whether the bubble spirals or zigzags when the Reynolds number exceeds a threshold. For example, Saffman observed only zigzagging bubbles using filtered water [12], while Miyagi [11], Aybers & Tapucu [14] observed only spiralling bubbles(water type not specified), in the bubble diameter regime d $<$ 0.2 cm. Our experiments demonstrate that the path of the bubble is sensitive to its shape. For nearly spherical bubbles (or bubbles generated by

gentle-push method), the straight path of the bubble is changed to a zigzag path (Fig. (5a)). For ellipsoidal bubbles (or bubbles generated by pinch-off method), a straight path of the bubble is changed to a spiral path (see Fig. (5b)). These experimental results resolve the disagreements mentioned above. Saffman used a gentle-push method in which a capillary of inner diameter of 0.16 cm was used [12], thus only zigzagging bubbles were observed. On the other hand, Miyagi used a pinch-off method [11], thus only spiralling bubbles were observed. Unfortunately, generation method was not mentioned in the report of Aybers & Tapucu [14], although their experimental results indicate that a pinch-off method was used.

To further strengthen the finding that air bubbles in this diameter regime have bistable shape states, a sphere and an ellipsoid, a simple test was carried out. In this test, an ellipsoidal bubble ($\chi = 2.1$) of diameter of 0.20 cm was found to change into a spherical one ($\chi = 1.04$) when it was sufficiently perturbed by an obstacle placed along its path. The ellipsoidal bubble was generated by the pinch-off method, and then it was stopped by a 0.2 cm diameter circular hole in an 1/8" thick acrylic plate placed $\sim$ 2 cm above the needle tip. When the bubble was released by a gentle tap on the acrylic plate, it zigzagged at a velocity of 16 cm /s. On the other hand, it stayed in its ellipsoidal shape and spiralled at 34 cm /s when the acrylic plate was removed.

The experimental results presented here are consistent with previous findings that bubbles rise at a much slower rate in contaminated water. It is observed in experiments of Fdhila and Duineveld [6] as well as a few tests conducted in our lab that bubbles in the diameter regime of 0.1 - 0.2 cm are always spherical in shape in contaminated water, regardless of its generation mechanism. Systematic studies of the effects of contaminations on the shape of the bubbles are in progress.

It needs to be noted that there is no set criterion for cleanness of water in the current literature. Surface tension, though the best criterion so far, is not sensitive enough for this application. The clean water in this Letter refers to the water treated with the method described above, and specifications given. The contaminated water refers to water saturated with contaminants. It is known that the bubble velocity decreases with the increase of the

concentration of the contaminants until a threshold is reached [6].

We would like to thank Professor P. G. Saffman for insightful discussions and encouragement on the subject. We acknowledge Erin Englert and Ben Welander for their help during experimental work. Wu wishes to thank members of Gharib's group who offered generous help during her stay at Caltech. This work is supported by the Office of Naval Research (N00014-98-1-0017), the Petroleum Research Fund (ACS-PRF# 32904-GB9) and the Research Corporation (CC4612).

FIGURES

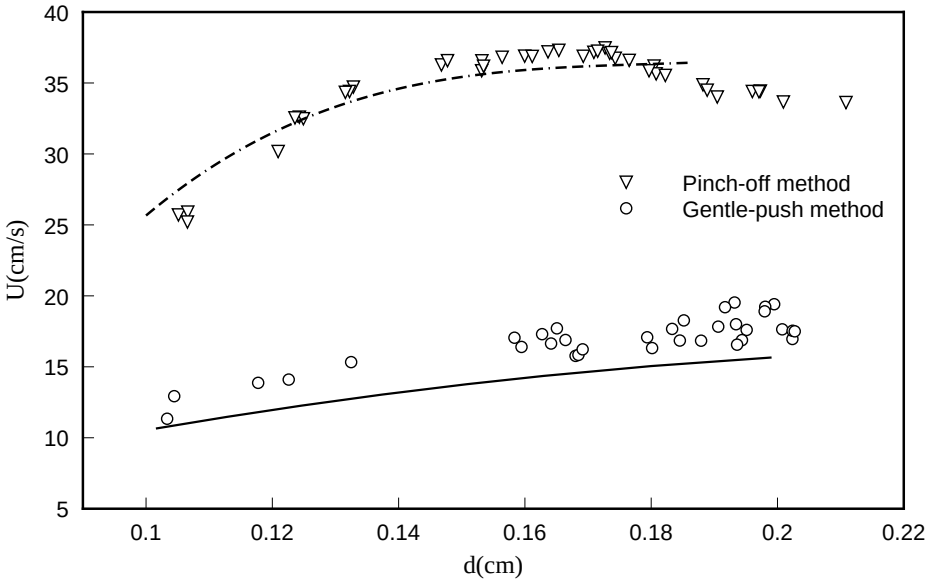

FIG. 1. Vertical terminal velocity U versus diameter d of bubbles generated by a pinch-off method $\bigtriangledown$; and a gentle-push method $\bigcirc$. The upper dashed line is data taken in clean water by Duineveld [5], and the lower solid line is data taken in contaminated water from Ref. [1].

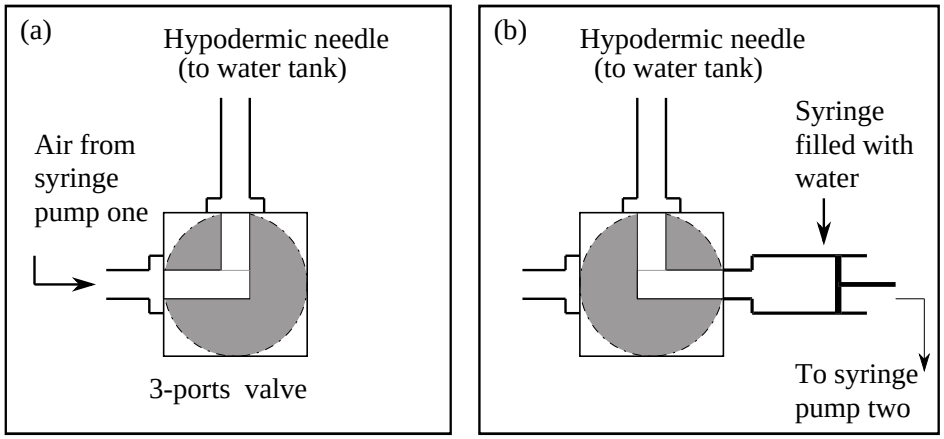

FIG. 2. Schematics of bubble generation mechanism.

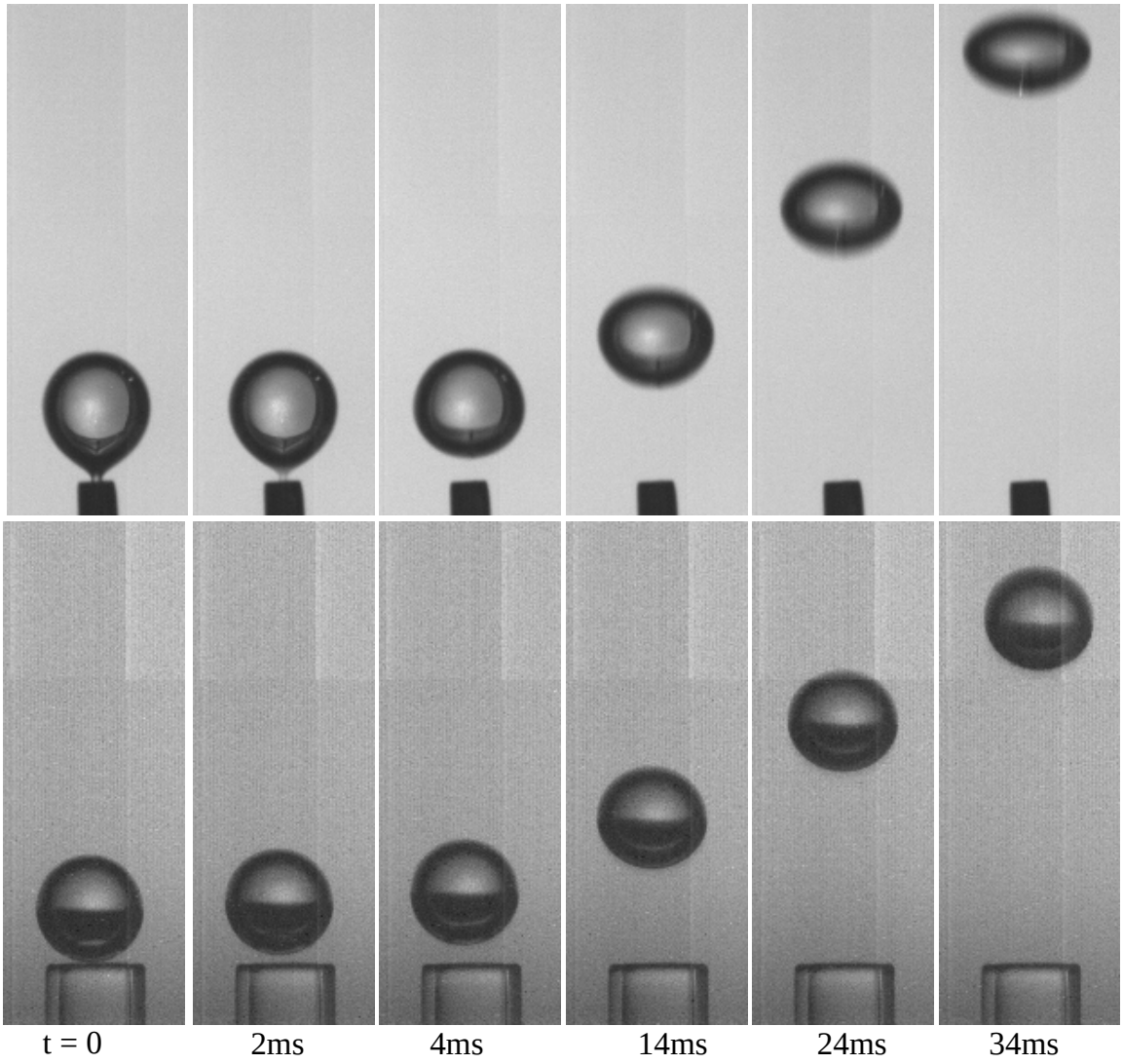

FIG. 3. Images of bubbles at detachment. The size of each image is 0.32 cm × 0.88 cm. Upper row: pinch-off method; lower row: gentle-push method.

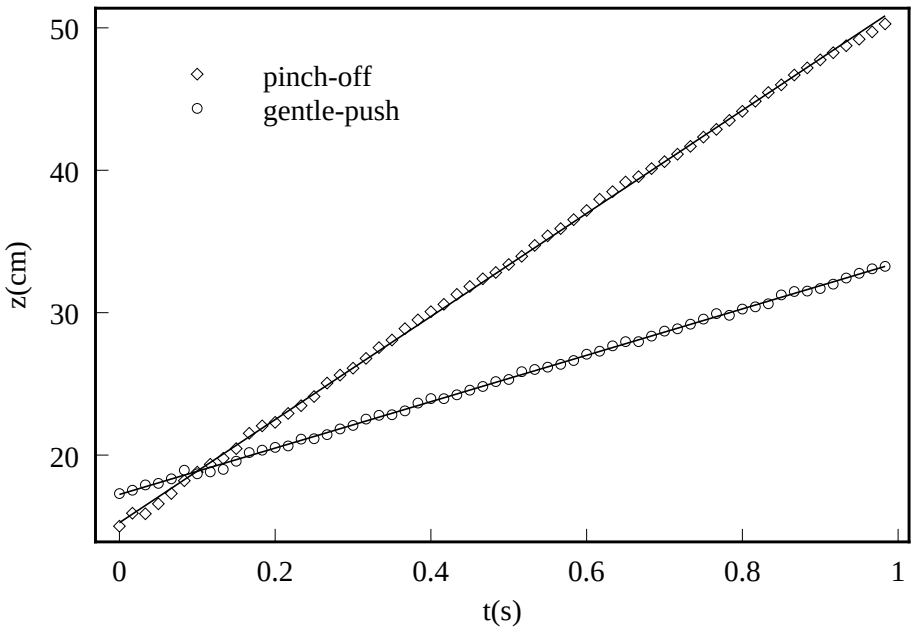

FIG. 4. Vertical displacement z of the rising bubble versus time t. $\circ$: data of a nearly spherical bubble generated by a gentle-push method. $\diamond$: data of an ellipsoidal bubble generated by a pinch-off method. Solid lines are fits to linear functions. The vertical velocity of the spherical bubble is $16.3cm/s$, and the ellipsoidal bubble is 36.2cm/s. The diameter of the bubbles in both cases is $d = 0.180cm$.

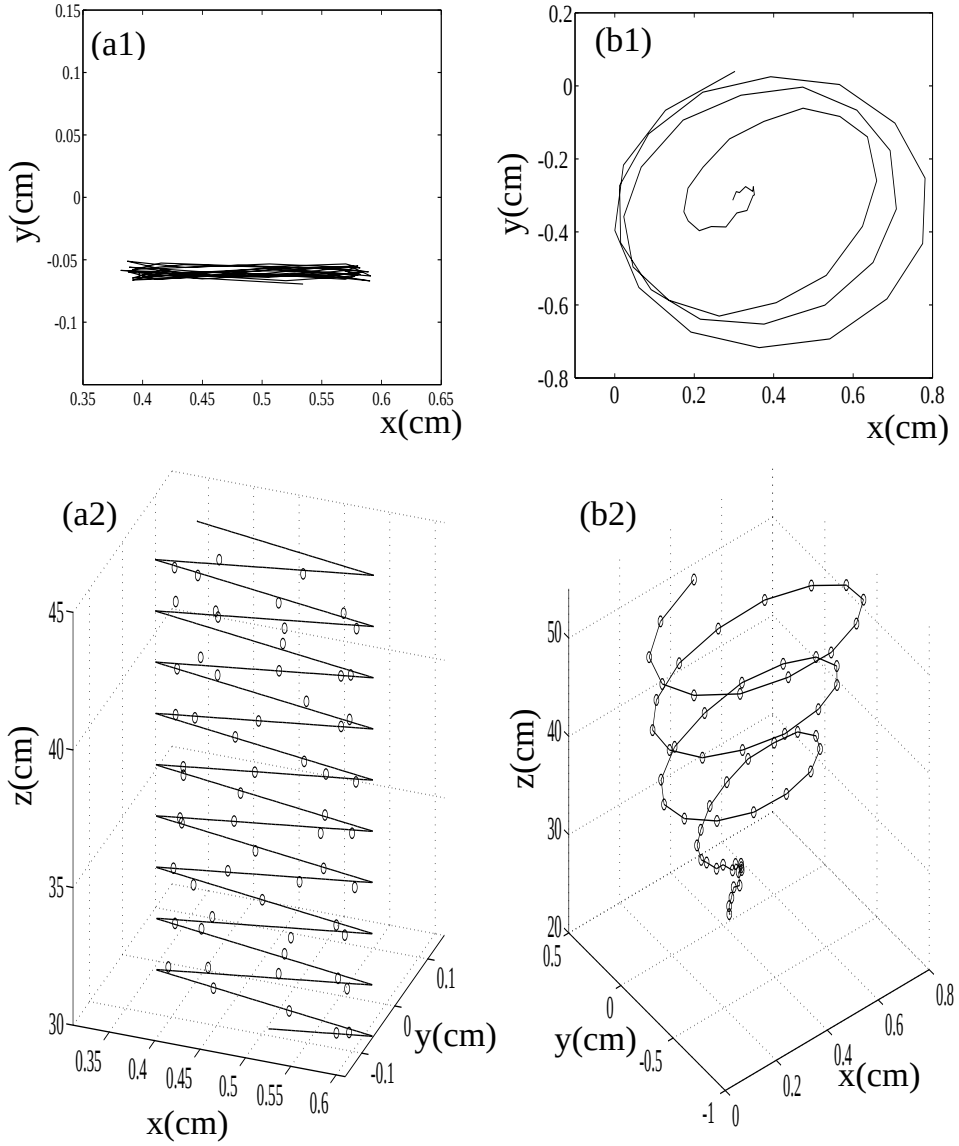

FIG. 5. a1(b1): Top view of the measured zigzag(spiral) path. a2(b2): 3D rendition of the zigzag(spiral) path. Circles are experimental data, solid line in (a2) is a fit to a zigzag function, in (b2) is a guided line. The equivalent diameter of both bubbles is 0.180 cm.

REFERENCES

[1] R. Clift, J. R. Grace and M. E. Weber, *Bubbles, Drops and Particles*, (Academic, 1978).

[2] J. Magnaudet, I. Eames, Annu. Rev. Fluid Mech. **32**, 659(2000).

[3] John Happel and Howard Brenner, *Low Reynolds Number Hydrodynamics*, 2nd edition, (Noordhoff International Publishing, Leiden, 1973).

[4] D. Ormiéres and M. Provansal, Phys. Rev. Lett., **83**, 80(1999).

[5] G. Ryskin, L. G. Leal, J. Fluid Mech. **148**, 19 (1984).

[6] R. Bel Fdhila, P. C. Duineveld, Phys. of Fluids **8**, 310(1996).

[7] W. L. Haberman and R. K. Morton, David Taylor Model Basin Report 802, 1953.

[8] P. C. Duineveld, J. Fluid Mech. **292**, 325(1995).

[9] C. E. Willert and M. Gharib, Experiments in Fluids **12**, 353 (1992).

[10] The Culligan water purification system consists of one carbon filter, two 0.45μm filters, one reverse osmosis system, two deionization columns, one UV water sterilizer and two 0.22 μm filters. The specific resistance of the water is 10 MΩ·cm.

[11] O. Miyagi, Technol. Rep. Tohoku Univ. **5**, 135(1925).

[12] P. G. Saffman, J. Fluid Mech. **1**, 249 (1956).

[13] R. A. Hartunian and W. R. Sears, J. Fluid Mech. **3**, 27 (1957).

[14] N. M. Aybers and A. Tapucu, Warme- und Stoffubertragung Bd. 2, 118(1969).

[15] T. Maxworthy, C. Gnann, M. Kürten and F. Durst, J. Fluid Mech. **321**, 421 (1996).

[16] K. Lunde and R. J. Perkins, Paper no. FEDSM97-3530, ASME-FED Summer Meeting, Vancouver, Canada , 1997.